Model-Based Optimization of Feeding Recipe for Rifamycin Fermentation

Prashant M. Bapat, Nitin U. Padiyar, Nishant N. Dave, Sharad Bhartiya, Pramod P. Wangikar
Dept. of Chemical Engineering, Indian Institute of Technology, Bombay, Powai, Mumbai 400 076, India

Sachi Dash
Automation and Control Solutions (ACS) Laboratory, Honeywell International, Phoenix, AZ 85027

DOI 10.1002/aic.11034
Published online November 2, 2006 in Wiley InterScience (www.interscience.wiley.com).

Industrial fermentation processes typically use complex media and operate in fed-batch mode to minimize the effects of catabolite repression. However, model-based feeding recipes have not been reported for such processes primarily as a result of the lack of reliable process models. By using a recently published process model, we optimize the feeding recipe for rifamycin B fermentation in complex media. Experimental validation shows a twofold improvement in productivity over an optimized batch. The dynamic optimization problem was posed as a nonlinear program and solved using successive quadratic programming. The feed profiles of four substrates were parameterized to convert the problem into a finite decision space consisting of substrate feed rates and switching intervals. Several distinct recipes, each corresponding to a unique initial guess of decision variables, showed comparable productivity, implying the presence of multiple local optima. The strategy presented here can be applied for optimization of other fermentation processes for which reliable process models are available. © 2006 American Institute of Chemical Engineers *AIChE J,* 52: 4248–4257, 2006

Keywords: sequential substrate utilization, cybernetic model, successive quadratic programming (SQP) solver

Introduction

The fermentation industry accounts for a few hundred billion dollars in sales annually. Fermentation products include ethanol, antibiotics, therapeutic proteins, and industrial enzymes. Thus the fermentation industry represents a cost competitive and raw material intensive operation. Fermentation operates normally in a high-volume range of 50 to 90 m^{31} and it is "cultivation cost intensive."[2] The large batch cycles, ranging from 1 to 15 days, require careful planning and control because blending of products from poor batches is not permitted as in other chemical industries such as polymer and petroleum. Despite the large stakes involved, operating policies in the fermentation industry are based on trial-and-error methods for optimizing and monitoring the fermentation batch.[3] Although these ad hoc methods work in practice, additional benefits may be realized through use of model-based tools such as optimization, fault diagnosis, monitoring, and control. A hurdle in use of such tools is the lack of availability of a reliable process model for the specific system. The desirable qualities of a fermentation model include an accurate representation of the various phases of growth, product formation, and substrate consumption. Further, the model should provide accurate predictions on a process time scale of several days.

In this work, we use a recently reported model for *Amycolatopsis mediterranei* to design optimal feed strategies for maximi-

P. P. Wangikar is also affiliated with the School of Bioscience and Bioengineering, Indian Institute of Technology, Bombay, Powai, Mumbai 400 076, India.
Correspondence concerning this article should be addressed to P. P. Wangikar at pramodw@iitb.ac.in or S. Bhartiya at bhartiya@che.iitb.ac.in.

zation of the antibiotic rifamycin B.[4] The rifamycins,[5] exemplified by rifamycin B, are a family of ansamycin antibiotics[6] with pronounced antimycobacterial activity that are extensively used in the clinical treatment of tuberculosis, leprosy, and AIDS-related mycobacterial infections.[7] The rifamycin B is produced by *Amycolatopsis mediterranei*[8] in complex medium containing glucose as a primary carbon source and ammonium sulfate (AMS) as a primary nitrogen source. Additionally, the medium contains defatted soya flour (DSF) and corn steep liquor (CSL), which may act as a substitutable carbon/nitrogen source. It is well known that the rifamycin B synthesis is inhibited by excess concentration of nitrogen and carbon substrates.[8]

Design of substrate feeding recipes to maximize production of rifamycin B during fed-batch fermentation can be posed as a dynamic optimization problem. Of the various approaches to solving the dynamic optimization problem, discretization of the input profiles and its subsequent conversion to a nonlinear program (NLP) have been widely reported for various applications including fermentation.[9-15] However, most of these reported applications deal with well-defined media and relatively short batch cycles. Further, very few reported cases attempt an experimental validation of the proposed optimal recipes. The present work involves growth on complex medium with a typical batch cycle of 200 h. In addition, the inputs also consist of complex media resembling industrial practice. Further, we present results of an experimental implementation of the optimal recipes.

The experimental methods, process model, and the optimization strategy are presented in the Experimental section, whereas the Results section details the optimization results, experimental implementation, and comparison with an optimal batch and an ad hoc feeding strategy.

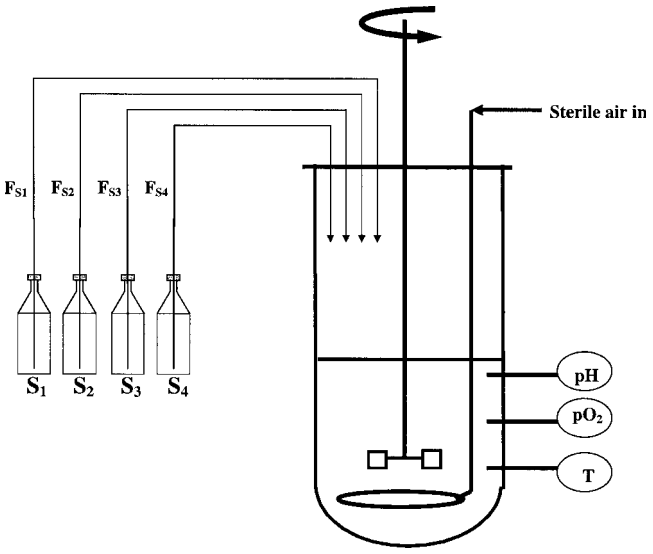

Figure 1. Representation of the bioreactor setup for fed-batch fermentation process.

The bioreactor is equipped with sensors for measuring temperature, pH, and dissolved oxygen concentration. The minimum volume is 1.5 L. The bioreactor is also equipped with analog peristaltic pumps to feed substrates with predetermined trajectories and a gas analyzer for measurement of oxygen and carbon dioxide fraction in the exhaust gas. S_1: amino acids; S_2: glucose; S_3: ammonia; S_4: insoluble nitrogen.

Experimental

Methods

Prof. Heinz Floss (Washington University, St. Louis, MO) kindly donated the rifamycin B overproducing strain of *Amycolatopsis mediterranei* S699 that does not require barbital.[16] The preculture was propagated as described by Kim et al.[17] About 150 ml of preculture (10% v/v) was used to inoculate the bioreactor. The media contained (per liter of distilled water) glucose, 80 g; potassium phosphate, 1 g; ammonium sulfate, 4 g; defatted soy flour (DSF), 8 g; corn steep liquor (CSL), 8 g; magnesium sulfate, 1 g; ferrous sulfate, 1 g; zinc sulfate, 0.010 g; and cobalt chloride, 0.0030 g. After adjusting the pH to 7.0 with 1 N sodium hydroxide, the fermentor was sterilized by autoclaving at 121°C for 15 min. Similarly, the feed bottles containing glucose 400 g L^{-1} and DSF–CSL 40 g L^{-1} were sterilized along with reactor. Care was taken to add a magnetic stir bar in the DSF–CSL bottle for better mixing during feeding.

Bioreactor and cultivation conditions

Figure 1 shows the typical bioreactor setup used for the rifamycin B production process. Batch cultivations were conducted in a 6.5-L BIOSTAT® B (B. Braun Biotech International, Schwarzenberger, Germany) bioreactor at a working volume of 1.50 L. The temperature was kept constant at 28°C and pH was monitored by maintenance-free autoclavable pH electrode (Ingold, Bel Air, MD). The dissolved oxygen (pO_2) during the fermentation run was measured by sterilizable polarographic pO_2 electrode (Ingold). An agitator was used as a control variable to maintain dissolved oxygen at 40% by cascade control. A mass flow controller (BBI Systems GmbH, Melsungen, Germany) supplied a constant airflow of 1.0 vvm (volume of air per volume of media). For the fed-batch operation, precalibrated programmable peristaltic feeding pumps (BBI Systems) were used. The trajectory of the feed was maintained by entering the feed rate values in the MFCS DA® software program (BBI Systems) interphased with a computer. The entire reactor assembly was kept on the weighing balance (Conweigh, Mumbai, India) to monitor total mass. Concentrations of O_2 and CO_2 in the exit gas stream from the bioreactor were measured by infrared spectroscopy and paramagnetic analysis, respectively (BINOS1002M® analyzer with sample conditioning unit, Rosemount Analytical Europe, Hasselroth, Germany).

Analytical techniques

Samples were drawn from the fermentation medium at regular intervals to analyze the dry cell weight and the concentrations of glucose, ammonium sulfate, free amino acids, and rifamycin B. Mycelia dry cell weight (DCW) was determined by first removing the insoluble substrates, which settle under gravity, and then filtering about 10 g cultivation medium on dried preweighed filters (Whatmann, Brentford, Middlesex, UK). The residue was washed with distilled water; the filter was dried to constant weight in a microwave oven (Kenstar Ltd., Mumbai, India) at 150 W for 4 min. Glucose was analyzed by refractive index (RI) detector in HPLC (Hitachi, Merck KgaA, Darmstadt, Germany) using an HP-Aminex-87-H column (BioRad, Hercules, CA) at 60°C. The mobile phase consists of

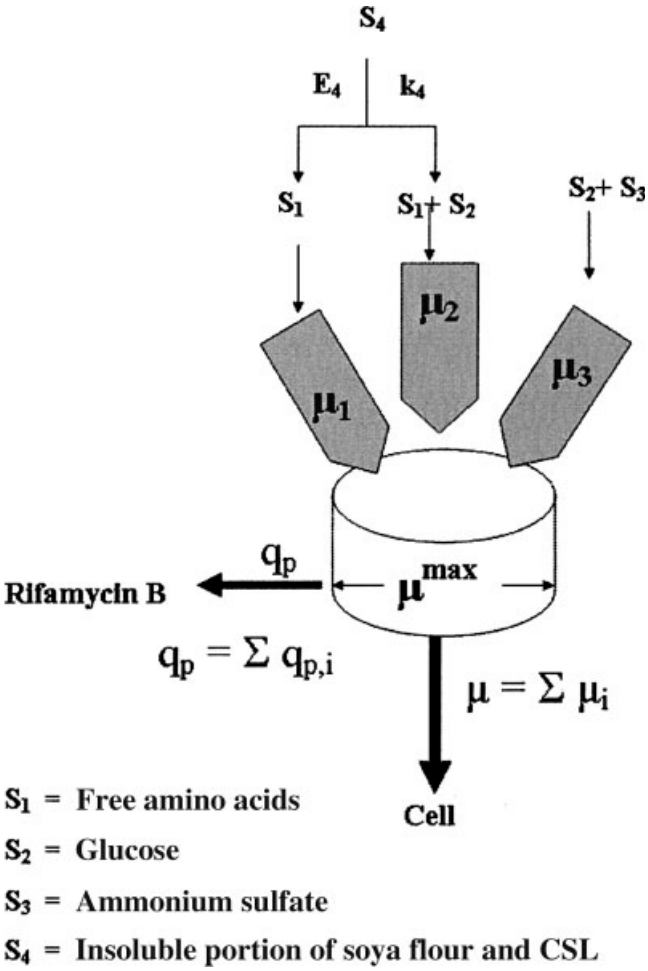

Figure 2. Representation of structured model in complex media.

The model assumes that the organism has access to up to three substrate combinations for growth. The organism prefers the substrate combination that gives maximum growth. The figure is adopted from previous work.[4]

HPLC-grade water (Millique, Millipore, Billerica, MA) with 5 mM sulfuric acid. An isocratic pump with a flow rate of 0.6 mL min^{-1} was used to resolute glucose from the fermentation broth. The concentration of free amino acids was estimated by the ninhydrin method.[18] Ammonium sulfate was determined by an ammonia-specific electrode (EA940 ion analyzer, Thermo Orion, Salem, MA). Rifamycin B was detected on spectrophotometer (model V-540, Jasco, Tokyo, Japan) at a wavelength of 425 nm as previously described.[19]

Process model for rifamycin B fermentation

Production of rifamycin B is the result of a series of primary and secondary metabolic reactions. Modeling rifamycin B is a challenge because of the long batch cycle and ill-defined nature of the media. A typical batch cycle time for rifamycin B is of the order of 7 to 9 days. A process model for rifamycin B was recently described in detail.[4] The model has been shown to account for the sequential uptake of substrates and the effects of nitrogen catabolite repression.[20] The model is based on cybernetic principles and assumes that the organism has access to up to three substrate combinations in complex medium:

(1) *Combination I*: pool of amino acids (S_1) (Eq. 1 for stoichiometry and growth rate on this substrate).

(2) *Combination II*: S_1 and glucose (S_2) (Eq. 2).

(3) *Combination III*: S_2 and AMS (S_3) (Eq. 3).

It is assumed that the free amino acids are released by hydrolysis of proteins and peptides (S_4) (Eq. 4). Equations 1–4 represent the four main growth reactions, with each equation consisting of the stoichiometry followed by the kinetic model form. The uptake of a substrate combination i is dependent on the level of the corresponding key enzyme (XEi), which may be inducible. Thus, the organism invests resources to synthesize XEi based on the growth achievable on the corresponding substrate combination. A schematic of the model is shown in Figure 2. The overall specific growth rate μ and specific production rate q_p are the weighted sums of the specific growth and production rates on the individual substrate combinations (Eqs. 10 and 16). The weights α_i are estimated using the optimality criteria (Eq. 10) in which the organism allows the uptake of all the substrate combinations as long as the specific growth rate obtained by summing the rates on different substrate combination is less than its intrinsic growth capacity denoted by μ^{max} (also see Figure 2). The complete model constitutes component mass balances represented by 10 ordinary differential equations (ODEs) (Eqs. 11–19) along with the optimality criteria stated in Eq. 10. The simulation exercise to predict growth, product formation, and substrate utilization was carried out by integrating the set of simultaneous differential equations as an initial value problem. The model parameters were obtained as described previously (Table1).[4] For greater details about the model and the model parameter estimation, refer to Bapat et al.[4] The model equations are summarized below.

Amino acid uptake

$$X - Y_{1,1}S_1 = 0 \qquad \mu_1 = \alpha_1 \mu_1^{\max} \left(\frac{X_{E_1}}{X_{E_i,\mathrm{Ref}}} \right) r_1^* \tag{1}$$

Glucose uptake

$$X - Y_{2,1}S_1 - Y_{2,2}S_2 = 0 \qquad \mu_2 = \alpha_2 \mu_2^{\max} \left(\frac{X_{E_2}}{X_{E_2,\mathrm{Ref}}} \right) r_2^* \tag{2}$$

AMS uptake

$$X - Y_{3,3}S_3 - Y_{3,2}S_2 = 0 \qquad \mu_3 = \alpha_3 \mu_3^{\max} \left(\frac{X_{E_3}}{X_{E_3,\mathrm{Ref}}} \right) r_3^* \tag{3}$$

Conversion of insoluble nitrogen to amino acids

$$S_1 - S_4 = 0 \quad r_{\mathrm{diss}} = \left(\frac{X_{E_4}}{X_{E_4,\mathrm{Ref}}} \right) r_4^* k_4 X \tag{4}$$

Rifamycin B production

$$P - Y_{5,1}S_1 - Y_{5,2}S_2 = 0 \quad qp_2 = \alpha_2 qp_2^{\max} \left(\frac{X_{E_2}}{X_{E_2,\mathrm{Ref}}} \right) r_2^*, p \tag{5}$$

$$P - Y_{6,3}S_3 - Y_{6,2}S_2 = 0 \quad qp_3 = \alpha_3 qp_3^{\max} \left(\frac{X_{E_3}}{X_{E_3,\mathrm{Ref}}} \right) r_3^*, p \tag{6}$$

Enzyme synthesis

$$X_{E_i} - X = 0 \qquad r_{E_i} = K_{E_i} r_i^* \qquad \text{for } i = 1, 2, 3 \tag{7}$$

$$X_{E_4} - X = 0 \qquad r_{E_4} = K_{E_4} r_4^* \tag{8}$$

Table 1. Model Parameters for Growth and Product Formation in Rifamycin B Fermentation Using the Strain *Amycolatopsis mediterranei

Media Composition	Growth Parameters							Product Formation Parameters						
	μ_i^{max} (h^{-1})	K_{si} ($g\,L^{-1}$)	K_{sj} ($g\,L^{-1}$)	K_{Ii} ($g\,L^{-1}$)	K_{Ij} ($g\,L^{-1}$)	$Y_{x/si}$ ($g\,g^{-1}$)	$Y_{x/sj}$ ($g\,g^{-1}$)	qp^{max} (h^{-1})	Kp_i ($g\,L^{-1}$)	Kp_j ($g\,L^{-1}$)	Kp_{Ii} ($g\,L^{-1}$)	Kp_{Ij} ($g\,L^{-1}$)	$Y_{p/xi}$ ($g\,g^{-1}$)	$Y_{p/xj}$ ($g\,g^{-1}$)
I**	0.030	0.30	—	—	—	0.41	—		—	—	—	—	—	—
II†	0.080††	25	0.45	100	125	0.40	1.70	0.019	25	0.45	80	125	0.30	1.7
III‡	0.155	15	1.40	100	4.50	0.55††	2.10††	0.0205	15	1.0	100	4.50	0.107	0.85

*Model parameters taken from previous report.[4] Besides this the initial enzyme concentrations are fixed at 0.9, 0.005, 0.005, and 0.05 for X_{E1}, X_{E2}, X_{E3}, and X_{E4} respectively. Further, these enzymes become degraded at the rate of 0.004 h^{-1}. The dissolution constant (K_4) is fixed at 0.01255 h^{-1}.
**Soy flour and corn steep liquor (S_i).
†Glucose (Si) and soya flour and corn steep liquor (S_j).
††Modified parameters estimated from various batch runs conducted on the reactor.
‡Glouse (S_i) + Ammonium sulfate (S_j).
‡‡Dissloution constant, K_4: 0.01255 h^{-1}.

Degradation of enzymes

$$X - X_{E_i} = 0 \qquad r_{\deg,i} = k_{\deg,i} X_{E_i} \qquad i = 1,2,3,4 \tag{9}$$

Optimality criteria

$$\max(\mu) \quad \text{s.t.} \begin{cases} 0 \le \alpha_i \le 1 \\ \text{and } \mu \le \mu_{\max} \end{cases} \tag{10}$$

where $\mu = \sum_{i=1}^{3} \alpha_i \mu_i$.

Mass balance equations

Biomass

$$\frac{d(XV)}{dt} = \mu XV \tag{11}$$

Amino Acids

$$\frac{d(S_1V)}{dt} = F_{S_1} C_{F_{S_2}} - [(y_{1,1}\mu_1)\alpha_1 + (y_{2,1}\mu_2 + y_{5,1} q_{P,2})\alpha_3] XV + k_4 \left(\frac{X_{E_1}}{X_{E_1,\text{Ref}}}\right)\left(\frac{S_4}{k_{S_4} + S_4}\right) XV \tag{12}$$

Glucose

$$\frac{d(S_2V)}{dt} = F_{S_2} C_{F_{S_2}} - [(y_{2,2}\mu_2 + y_{5,2} q_{P,2})\alpha_2 + (y_{3,2}\mu_3 + y_{6,2} q_{P,3})\alpha_3] XV \tag{13}$$

Ammonium sulfate

$$\frac{d(S_3V)}{dt} = F_{S_3} C_{F_{S_3}} - [y_{3,3}\mu_3 + y_{6,3} q_{P,3}]\alpha_3 XV \tag{14}$$

Insoluble nitrogen

$$\frac{d(S_4V)}{dt} = F_{S_4} C_{F_{S_4}} - [y_{1,1}\mu_1 + y_{2,1}\mu_2 + y_{5,1} q_{P,2}] XV + k_4 \left(\frac{X_{E_1}}{X_{E_1,\text{ref}}}\right)\left(\frac{S_4}{k_{S_4} + S_4}\right) X \tag{15}$$

Product

$$\frac{d(PV)}{dt} = q_p XV \tag{16}$$

where $q_p = \sum_{i=1}^{3} \alpha_i q_{p_i}$.

Enzymes

$$\frac{d\frac{X_{E_1}}{X_{E_1,\text{Ref}}}}{dt} = \left(\mu_i^{\max} + k_{\deg,i}\right) \frac{S_1}{S_2 + Ks_{1,t} + S_1 + \frac{S_1{}^2}{K_{11,1}}} - (\mu + k_{\deg,i}) \frac{X_{E_1}}{X_{E_1,\text{Ref}}} \tag{17}$$

$$\frac{d\frac{X_{E_i}}{X_{E_i,\text{Ref}}}}{dt} = \left(\mu_i^{\max} + k_{\deg,i}\right) r_i^* - (\mu + k_{\deg,i}) \frac{X_{E_i}}{X_{E_i,\text{Ref}}} \qquad (i = 2,3) \tag{18}$$

$$\frac{d\frac{X_{E_4}}{X_{E_4,\text{Ref}}}}{dt} = \left(\frac{\mu + k_{\deg,4}}{1 + \left(\frac{T_N}{W}\right)^d}\right) r_4^* - (\mu + k_{\deg,4}) \frac{X_{E_4}}{X_{E_4,\text{Ref}}} \tag{19}$$

where values of r_i indicate the effect of substrate limitation on growth and product formation and are based on Michelis–Menten kinetic form with multiple limiting substrates and substrate inhibition.[20]

Optimization strategy

The use of multiple substrates, complex media, and the long fermentation batch cycle (>1 week) necessitates developing optimal feed recipes that maximize the productivity in a fed batch. While familiarity with the different phenomena involved in the process provide guidelines in the design of the recipe, a superior strategy may be systematically found through a model-based dynamic optimization.[21] Moreover, formulation of the optimization problem enables rigorous satisfaction of various operating constraints such as maximum allowable feed rates, volume of fermentor, and maximum biomass concentration. A general formulation of the dynamic optimization problem can be stated as

$$\max_{u(t),t_F} J = P(t_f) \tag{20a}$$

$$\text{s.t. } \dot{\mathbf{x}} = f[\mathbf{u}(\mathbf{t}), \mathbf{x}(\mathbf{t})] \tag{20b}$$

$$\mathbf{x}(t_0) = \mathbf{x}_0 \tag{20c}$$

$$\begin{cases} \mathbf{x}_{\min} \le \mathbf{x}(t) \le \mathbf{x}_{\max} \\ \mathbf{u}_{\min} \le \mathbf{u}(t) \le \mathbf{u}_{\max} \end{cases} \tag{20d,e}$$

where t_0 and t_f denote the start and end of the fed-batch process, respectively, and $\mathbf{x}(t)$ and $\mathbf{u}(t)$ represent the state variables

Table 2. Physical Constraints Imposed on the Optimization Program Based on Aspects Such as Safety, Solubility of Substrates, Reactor Geometry, Pump Capacity, and Sensitivity of the Cells to Shear

Parameter	Unit	Min	Max	Fixed
Temperature	°C	—	—	28
Dissolved oxygen	%	—	—	40
C_{F_1}	g/L	—	—	30
C_{F_2}	g/L	—	—	400
C_{F_3}	g/L	—	—	30
C_{F_4}	g/L	—	—	30
Batch termination time (t_f)	h	180	210	
Air flow	vvm	—	—	1
Volume	l	1.5	2.5	—
Feed flow rates	1/h	0.0	0.75	—
Stirrer	RPM	180	650	—

and the inputs to the process, respectively. Equation 20b summarizes the process model discussed in the previous section (Eqs. 1–19). Thus, the state variables for the fermentation model are

$$\mathbf{x}^{\mathrm{t}} = \left[X \quad S_1 \quad S_2 \quad S_3 \quad S_4 \quad P \frac{X_{E_1}}{X_{E_1}^{\mathrm{Ref}}} \frac{X_{E_2}}{X_{E_2}^{\mathrm{Ref}}} \frac{X_{E_3}}{X_{E_3}^{\mathrm{Ref}}} \frac{X_{E_4}}{X_{E_4}^{\mathrm{Ref}}} \right] \tag{21}$$

The process inputs represent the feed rates of the four substrates. Thus

$$\mathrm{u}_t = [F_1 \quad F_2 \quad F_3 \quad F_4] \tag{22}$$

Equation 20d represents process- and safety-related constraints on the states and the inputs. The various state and feed constraints used in the current work are documented in Table 2. The solution of the above optimization problem yields the optimal feeding strategy.

Among the various methods for solving the dynamic optimization problem (Eq. 20), the approach consisting of parameterizing the control vector **u** and subsequently casting the dynamic optimization problem to a *nonlinear program* (NLP) and is well suited to large-scale problems.[22–25] This method is also known as *control vector parameterization* (CVP). An additional advantage of NLP methods is the availability of efficient NLP solvers. In the CVP approach, only the input **u** is parameterized and the states and objective function are evaluated by solving the dynamic equations. The input profiles may be approximated using a series of piecewise polynomials, γ, and associated input parameters as follows:

$$u_i(t) = \sum_{j=1}^{na} a_{ij}\, \gamma_{ij}\, (t - t_{ij}) \tag{23}$$

where t_{ij} is the jth switching time of the ith manipulated variable, na is the number of switching intervals, and a_{ij} represents the amplitude of the ith manipulated variable at the switching time t_{ij}. We make use of a zero-order trial function, wherein the feed rate is held constant in a particular interval i. Given the set of control parameters and initial conditions, the process model can be integrated using an ODE solver.[26–30]

In the current work, apart from the amplitude of the input, a_{ij}, we have also optimized switching intervals t_{ij}, which determine the time at which the amplitude of the input is changed. We used 10 switching intervals for each of the flow rates, making a total of 76 decision variables (9 amplitudes and 10 switching intervals for each of the four feed rates).

The resulting NLP can be stated as follows:

$$\max_{a_{ij}, t_{ij}} \; P(t_f) \tag{24}$$

$$\left.\begin{aligned} a_{ij\,\min} \le a_{ij} \le a_{ij\,\max} \\ \text{s.t.} t_{ij\,\min} \le t_{ij} \le t_{ij\,\max} \\ t_{f\,\min} \le t \le t_{fj\,\max} \end{aligned}\right\} \quad i = 1,4,\; j = 1,10 \tag{25}$$

where $P(t_f)$ represents the product at the end of the batch cycle and is found through integration of Eqs. 1–19. The constraints are summarized in Table 2. We used the *fmincon* function available in MATLAB® (The MathWorks, Natick, MA), a standard successive quadratic programming (SQP) solver, to obtain the optimal profiles.[31,32]

Results

The parameters of the process model are listed in Table 1. The parameters were estimated from the various batch runs conducted on the fermentor with initial media composition consisting of (1) glucose as a carbon substrate and ammonia as nitrogen substrate; (2) glucose as carbon substrate and mixture of soya and corn steep liquor as nitrogen substrate; and (3) glucose as carbon substrate and ammonia, soya, and corn steep liquor as nitrogen substrate. The parameter values were similar to those reported earlier for shake flask[4] with the exception of k_4, $\mu_2^{\max}$, $y_{3,2}$, and $y_{3,3}$. The practical constraints on the substrate feeding recipes are listed in Table 2. The important constraints were in terms of the working volumes in the fermentor and the feed flow rates. Note that these constraints (Table 2) were specific to the reactor vessel and the feeding pumps that were used in our work. Similarly, the process model parameters (Table 1) were specific to the strain of *Amycolatapsis mediterrnaei* S699 used in this study.

Improvement in productivity by model-based optimization

As discussed in the Experimental section, the SQP optimization algorithm was used to solve the NLP of Eqs. 24 and 25. The optimization resulted in distinct feed recipes, each corresponding to a unique initial guess of the decision variable. We have verified that the difference between each of these optima is not the result of convergence tolerances of the objective function and decision variables used by the SQP solver. Interestingly, each of these solutions produced a comparable value of the final product concentration. This implies the presence of many local optima in the decision space consisting of recipes with similar objective function values. We selected one of the optimum recipes for experimental verification (Figure 3). The recipe involves the feeding glucose solution (FS2) and a suspension of defatted soybean flour and corn steep liquor (DSF–CSL) (FS4). The corresponding optimum batch time was found to be 210 h. The model predicted the product concentration at the end of fed-batch fermentation to be 8.9 g/L (Figure 4D). Upon implementing the optimal recipe, the experimental measurements show that the rifamycin B concentration was 7.2 g/L at 200 h. To quantify the benefit of optimization, we compared the results with three different cases (Figures 4A to 4C). Case I

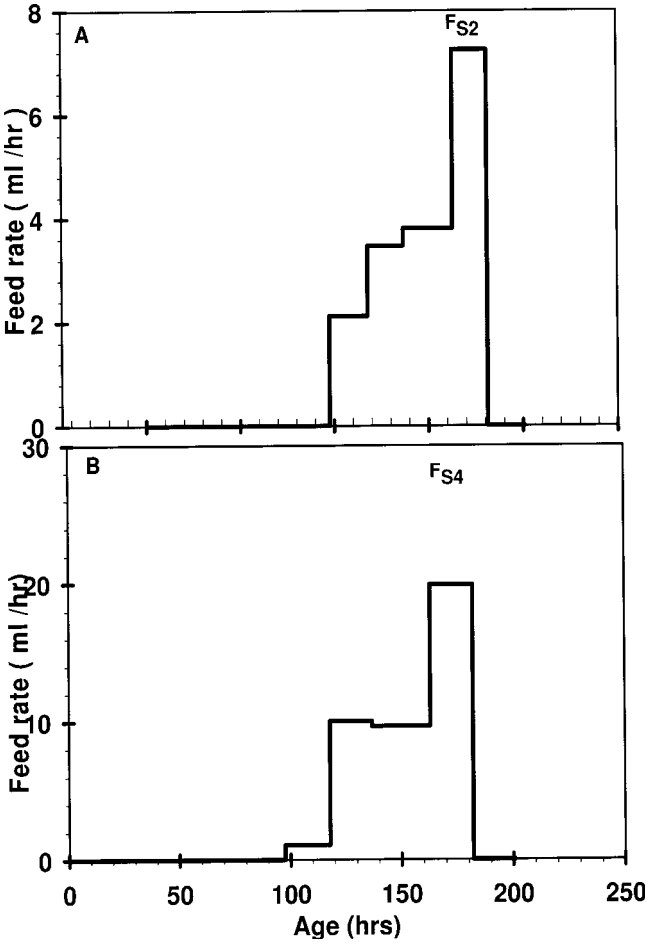

Figure 3. Optimal recipe implemented for experimental validation.

The optimum recipe consisted of feed flow rate trajectories for glucose (FS2) and insoluble organic nitrogen (FS4). The recipe was implemented by programming the peristaltic pumps.

consisted of a batch run where the initial media composition was optimized.[33] However, it was observed that the nitrogen substrate become limiting at 145 h. Case II and Case III consisted of fed-batch runs where the feeding recipe was synthesized based on the qualitative rationale of supplementing the carbon and nitrogen substrates with intermittent shots. The Case II recipe (see Table 3) was based on maintaining the carbon levels but faced nitrogen limitation similar to that in test Case I. Thus Case III was based on intermittent shots of glucose and organic nitrogen substrate (Table 3).

Experimental implementation of these cases reveals that the optimized fed-batch recipe yields a 266% improvement in productivity over Cases I, II, and III (see Table 4). Cases I and II were expected to provide a lower productivity as a result of the substrate limitations. However, Case III was found to provide lower productivity despite the fact that substrate limitation was accounted for in the feeding recipe. This implies that the empirically designed Case III did not account for the nitrogen catabolite repression, thereby resulting in a lower productivity. However, the nitrogen catabolite repression has been captured by the process model. It is thus expected that the model-based optimized recipe will ensure feeding to circumvent repression.

We had access to different process variables during the fed-batch run. These may be classified as off-line measurements such as substrate and product concentration and on-line measurement such as pH, CO_2 evolution rate, and dissolved O_2 concentration. The model accounts for a few of these variables. The collective information enabled tracking of the various phenomena occurring during the batch.

Modeled variables and model fit

The model parameters were estimated by a well-designed experimental plan involving batch runs.[20] Here, the model was used to predict dynamic profiles of the substrate, product and biomass concentrations, and the levels of enzymes for a specific feeding recipe. Note that the enzyme concentrations have not been measured. The model-predicted and the measured concentrations of rifamycin B during the course of the fed batch are shown in Figure 4. It is observed that the model accurately captures the product and substrate concentrations until about 120 h. Beyond 120 h, the model overpredicts the substrate consumption and product formation rates. Thus it is seen from Figure 4D that predicted rifamycin B concentration is higher than the measured concentration, particularly beyond 120 h. The model deviation was concomitant with a sharp rise in viscosity (data not shown). This may potentially lead to mass transfer limitation for the oxygen substrate, which has not been modeled. This is a possible reason for the overprediction of the rates of reaction.

We observed that the fermentation of *Amycolatapsis mediterrnaei* S699 in multisubstrate complex medium may be characterized by three distinct phases. During the first 30 h amino acids are used as a sole source of carbon and nitrogen (Figure 5C). Between 30 and 75 h, glucose is used as the primary carbon source and AMS as primary nitrogen source (Figures 5A and 5B). These phases are marked with high growth rate. From 75 h onward glucose and amino acids play the role of primary carbon and nitrogen substrate, respectively. Note that the highest product formation occurs in this phase.

On-line measurements

In addition to the modeled variables, we measured pH, dissolved oxygen, and CO_2 evolution rate as shown in Figure 5D. Although these variables are not modeled they provide additional information and may be correlated with the three distinct phases.[34] The pH trend reflects the nature of the nitrogen substrate being consumed. For example, between 0 and 30 h, an increasing pH trend coincides with consumption of amino acids as sole source of carbon and nitrogen. The subsequent decreasing pH trend coincides with phase where AMS is consumed as the primary nitrogen source. The increasing pH trend in the third phase again reflects the consumption of amino acids as the nitrogen source. The rate of CO_2 evolution (qCO2) is proportional to the rate of respiration by the cell mass. The respiration may be a result of growth or maintenance. The rapid increase in the rate of CO_2 evolution coincides with high growth between 0 and 100 h. Subsequently, the growth rate slows down, which is reflected in the steady CO_2 evolution rate. Based on the preliminary studies it was found that pO_2 at 40% of saturation value was necessary to eliminate dissolved

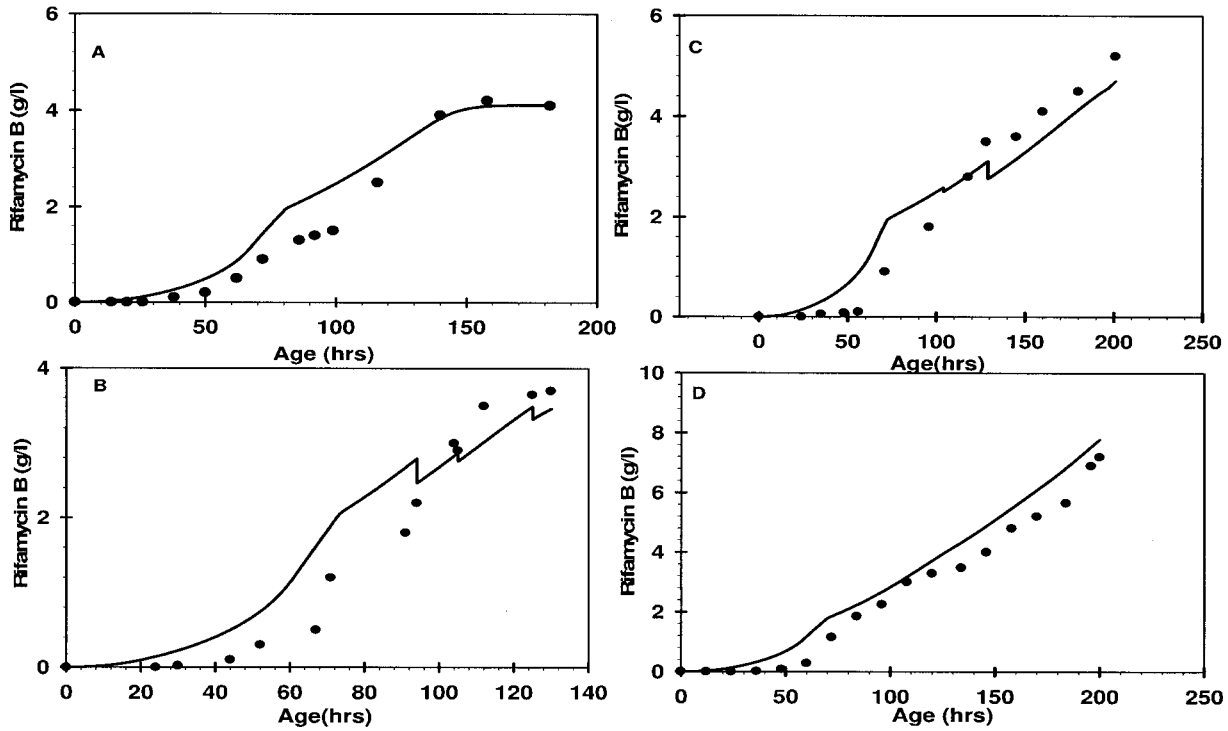

Figure 4. Rifamycin B concentration profile in optimized batch and comparison with Cases I, II, and III.

The solid line represents model prediction for the concentration of rifamycin B. (A) Feeding recipe obtained by model based optimization. Refer to Figure 3 for feed profile. (B) Case I: optimized batch. (C) Case II: fed-batch with glucose feed. (D) Case III: fed-batch with glucose and insoluble organic nitrogen substrate. Refer to Table 3 for initial charge and feed profiles for Case II and Case III.

oxygen limitation. The pO_2 levels were controlled by cascading with agitation rate. Thus, the agitator speed is governed by the O_2 demand as well as the mass-transfer coefficient. Note that the mass-transfer coefficient may change during the batch cycle because of the substrate feeding and change in viscosity. The 40% pO_2 required could be implemented until nearly 100 h, beyond which the agitation requirement was greater than the motor capacity. This is consonant with the sharp rise in viscosity. Thus, the pO_2 set point was reduced to 30% at 100 h and subsequently 20% at 180 h. The reduced pO_2 levels may cause O_2 to become the rate-limiting substrate. Because O_2 substrate was not modeled, this may partially explain the deviation between model predicted and measured values.

Discussion

Model-based optimization of feeding recipe for antibiotic fermentation has been a challenge, mainly arising from the lack of a reliable process model. This article presents, for the first time, a model-based optimization of multisubstrate feeding strategy including the feeding of organic nitrogen substrate. We used a recently reported process model for rifamycin B fermentation[4] that accounts for sequential uptake of substrates in a multisubstrate environment. Further, the model is able to accurately represent the nitrogen catabolite repression. This is effectively reflected in the substantial improvement in product that we obtain with an optimized feeding strategy. It may be noted that the optimum feeding strategy aims at achieving high growth within the first 100-h phase followed by a slow growth but a high product formation rate.

It may be noted that the optimization algorithm used here tries to find a local optimum in the decision variable space. The optimum obtained may be dependent on the initial guess value of the feeding recipe provided to the optimizer. We found multiple distinct recipes that give comparable final concentrations of rifamycin B. Two of the representative recipes are shown in Figures 6 and 7. Note that all the recipes include the feeding of glucose (FS2). Moreover the glucose feed starts at about 100 h in all the recipes including the one implemented (as shown in Figure 3A). The nitrogen substrate feed, on the other hand, differs significantly from recipe to recipe. For example, the recipe shown in Figure 6A feeds amino acids (FS1), whereas the recipe in Figures 7B and 7C feeds AMS (FS3) and insoluble or-

Table 3. Nutrient Shots Given in Cases I, II and III*

Case	Time of shot (h)	Glucose Shot (mL)	Organic Nitrogen Substrate Shot** (mL)
I	—	—	—
II	94	200	—
	105	80	—
	125	100	—
III	104	—	50
	129	200	—

*The initial charge for Cases I, II, III and optimized fed-batch includes, amino acids: 4 g/L; glucose: 80 g/L; AMS: 4 g/L; and organic nitrogen substrate: 16 g/L. The concentration of other media components were used as reported previously.[32]

**Glucose (400 g/L) and organic nitrogen substrate[DSF (15 g/L) + CSL (15 g/L)] were used to give nutrient shots.

Table 4. Improvement in Rifamycin B Productivity during Substrate Feed Optimization

	Age (h)	Rifamycin B(g/L)	Volume (L)	Rifamycin B(g)	Productivity Factor (PF) ($g/L^{-1}/h^{-1}$)	Improvement in PF* (%)
Case I	140	4.0	1.50	6.00	0.038	100*
Case II	150	3.70	1.86	6.88	0.049	128
Case III	200	5.20	1.74	9.00	0.041	108
Optimized fedbatch	200	7.20	2.80	20.2	0.101	266

*Productivity of Case I was taken as 100% to compare improvement in productivity with that of other batches.

ganic nitrogen (FS4), respectively. Moreover, the amount of nitrogen fed is different in those recipes. This may be attributable to the differences in the nitrogen catabolite repression exerted by ammonium sulfate and free amino acids. Of the competing recipes generated by the optimization algorithm, we implemented the recipe that feeds glucose along with organic nitrogen substrate (shown in Figures 3A and 3B) over the recipes that feed AMS or amino acids (Figures 6A and 7B). This was done to minimize the effect of model error, if any, on the product formation during the feeding phase. A small error in the model may result in the accumulation of nitrogen substrate, thereby exhibiting nitrogen catabolite repression. The insoluble nitrogen substrate, on the other hand, releases the nitrogen substrate in the form of free amino acids. This sustained release would help minimize the nitrogen catabolite repression even in the presence of a model error.

We observed some deviation between model-predicted and experimentally measured variable values for the optimized fed-batch run. Specifically, the model overpredicted the rates of product formation and substrate use after 120 h. This discrepancy may be attributed to the oxygen limitation, which has not been accounted for in the model. It may be possible to account for this in the model by incorporating oxygen as one of the limiting substrates. The dissolved oxygen concentration can then be linked to the hydrodynamic parameters of the fermenter by using the relevant mass-transfer correlations.

The initial substrate concentrations were decided based on the prior work on optimization of product in a batch culture.[33] Thus the decision variables for optimization included only the feeding rates and switching intervals and the batch time. Note that the initial conditions can be incorporated as additional decision variables in our optimization formulation. In addition, the initial state of the culture plays an important role in deciding the fate of the batch. This initial state is parameterized in the form of initial enzyme levels, XEi, in the process model. The initial state of the culture in production stage fermentation

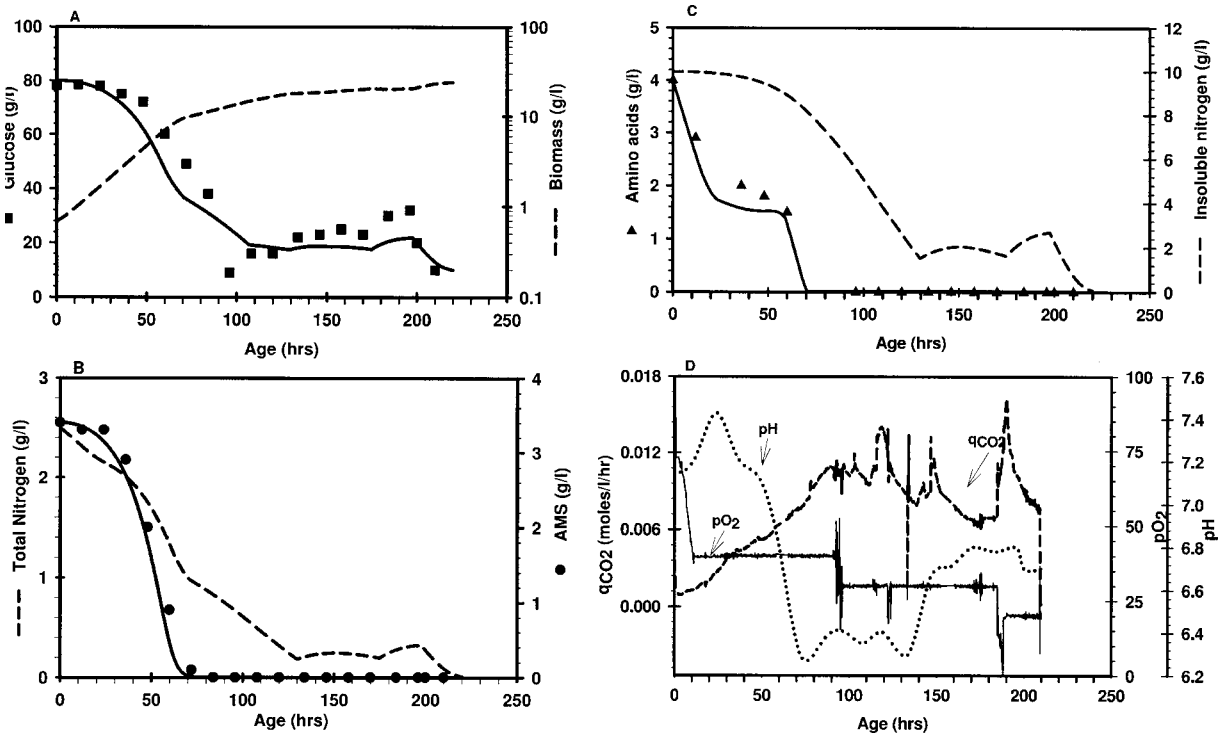

Figure 5. Model prediction and experimental measurements obtained during the experimental implementation of optimized feeding recipes shown in Figure 3.

Panels 3A, 3B and 3C, continuous and dashed lines represent model prediction, while panel 3D shows online measurements from the bioreactor.

is the final state of the culture in the preculture vessel. Thus, it may be possible to include the initial state of the culture in the form of XEi in the suite of decision variables in optimization. On a practical level, a given initial state of the culture may be achieved by changing the preculturing conditions and/or the seed transfer criteria.

Batch-to-batch variability in productivity can be a concern while implementing such feeding recipes. We conducted our experiments under relatively well controlled laboratory conditions and obtained reproducibility within 10% in replicate runs. However, variability may be unavoidable and could be an important issue for industrial-scale applications. Note that the monitoring and control of batch-to-batch variability in fermentation processes is beyond the scope of the present work and the interested reader may refer to works by Flores-Cerrillo and MacGregor[35] and Zhang and Lennox[36] for a detailed treatment of this topic.

The optimized recipes proposed here are specific to the strain of the microorganism and the fermentor vessel that we used. The strain of microorganism is parameterized in the form of the model parameters, whereas the fermentor vessel is parameterized in the form of the practical constraints imposed on the optimizer. It would be possible to generate optimal feeding recipes for other products/organisms by using a different process model or the relevant model parameters. Likewise, recipes may be generated for a larger-scale vessel by imposing a different set of practical constraints. Thus, the strategy of optimized substrate feeding recipe presented here may be applicable to other fermentation products of industrial importance.

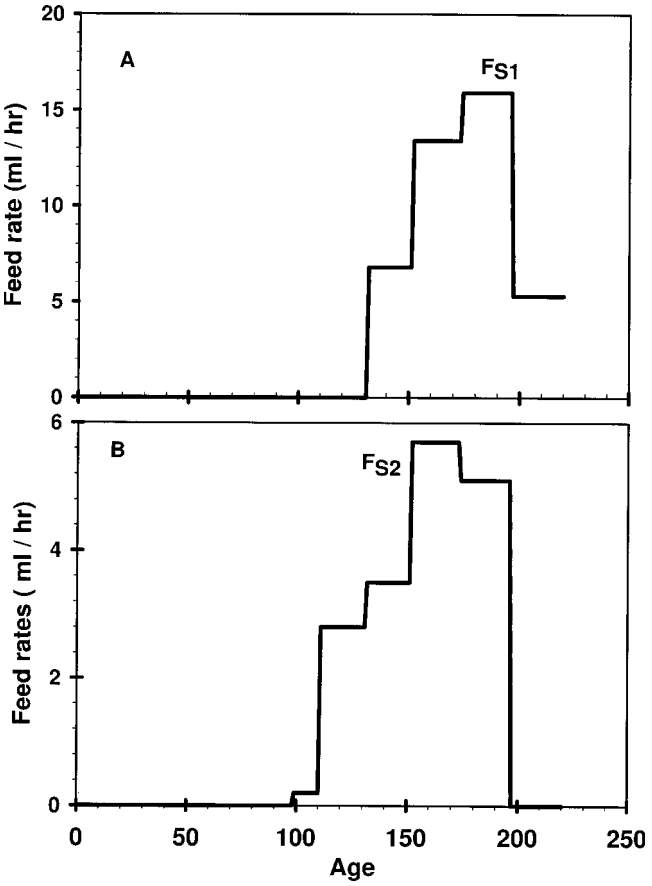

Figure 6. Competing feeding recipes generated through optimization algorithm.

Because of the presence of multiple local optima in the decision space of recipes, several recipes were generated by the optimization algorithm. Two examples are presented in A and B. For nomenclature refer to Figure 1.

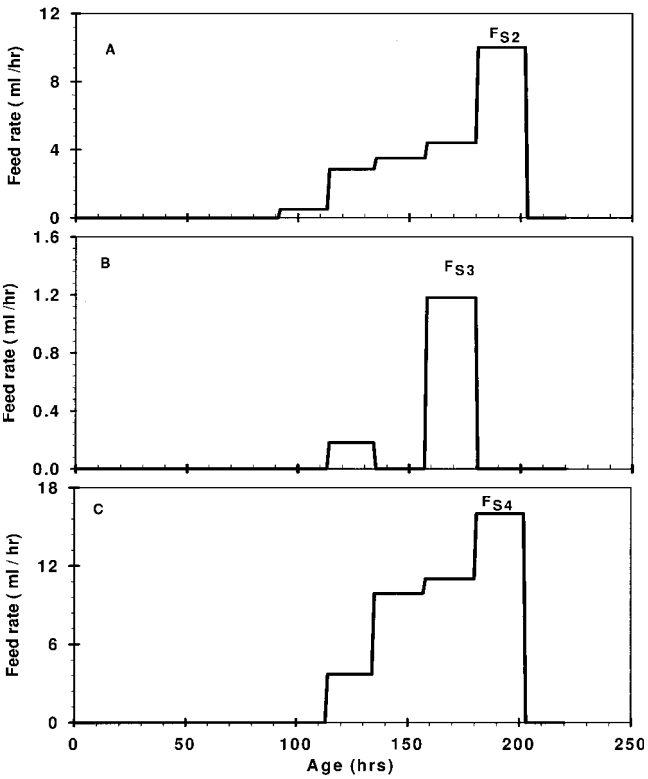

Figure 7. Competing feeding recipe II generated through optimization algorithm: for nomenclature, refer to Figure 1.

Acknowledgments

This work was partially funded by Honeywell International through Grant No. DRD/CL/SB-1/03-04.

Notation

$Ks_{m,j}$ and $Kp_{m,j}S_1$ = pool of amino acids, g L^{-1}
S_2 = glucose, g L^{-1}
S_3 = ammonium sulfate, g L^{-1}
S_4 = insoluble nitrogen substrate, g L^{-1}
μ_1^{max} = specific growth rate on S_1, h^{-1}
μ_2^{max} = specific growth rate on S_2 and S_1, h^{-1}
μ_3^{max} = specific growth rate on S_2 and S_3, h^{-1}
XEi = concentration of the enzyme responsible for uptake of substrate combination i
$K_{deg,i}$ = degradation constant for the enzyme E_i, h^{-1}
FSi = volumetric flow rate of feed containing substrate i, L h^{-1}
CFSi = concentration of substrate i used in the feeding, g L^{-1}
V = volume of liquid in the bioreactor, L
$Ks_{i,j}$ and $Kp_{i,j}$ = substrate half saturation constant for substrate j in the model for reaction i, g L^{-1}

$Y_{i,j}$ = stoichiometric coefficient of substrate j in reaction i, g g^{-1}
r_{diss} = dissolution rate of UNS to ANS (American Nuclear Standard) conversion, h^{-1}
qCO2 = carbon dioxide evolution rate, mole L^{-1} h^{-1}

Literature Cited

1. Jin ZH, Lin JP, Cen PL. Scale-up of rifamycin B fermentation with *Amycolatoposis mediterranei*. *J Zhejiang Univ Sci*. 2004;5:1590–1596.
2. Nielsen J. *Physiological Engineering Aspects of Penicillium chrysogenum*. Hackensack, NJ:World Scientific Publishing; 1997.
3. van Impe JF, Bastin G. Optimal adaptive control of fed-batch fermentation processes. *Control Eng Pract*. 1995;3:939–954.
4. Bapat PM, Bhartiya S, Venkatesh KV, Wangikar PP. Structured kinetic model to represent the utilization of multiple substrates in complex media during rifamycin B fermentation. *Biotechnol Bioeng*. 2006;93: 779–790.
5. Oppolzer W, Prelog V. The constitution and configuration of rifamycins B, O, S and SV. *Helv Chim Acta*. 1973;56:2287–2314.
6. Rinehart KL Jr, Shield LS. Chemistry of the ansamycin antibiotics. *Fortsch Chem Organ Naturst Prog Chem Organ Nat Products Prog Chim Subst Organ Nat*. 1976;33:231–307.
7. Sepkowitz KA, Raffalli J, Riley L, Kiehn TE, Armstrong D. Tuberculosis in the AIDS era. *Clin Microbiol Rev*. 1995;8:180–199.
8. Sensi P, Margalis P, Timbal M. Rifamycin, a new antibiotic: Preliminary report. *Farm Ed Sci*. 1959;14:146–147.
9. Birol G, Undey C, Cinar A. A modular simulation package for fed-batch fermentation: Penicillin production. *Comput Chem Eng*. 2002; 26:1553–1565.
10. Guthke R, Knorre A. Optimal substrate profile for antibiotic fermentations. *Biotechnol Bioeng*. 1981;23:2771–2777.
11. Johnson A. The control of fed-batch fermentation processes—A survey. *Automatica*. 1987;23:691–705.
12. Lee J, Lee SY, Park S, Middelberg APJ. Control of fed-batch fermentations. *Biotechnol Adv*. 1999;17:29–48.
13. Modak JM, Lim HC, Tayeb YJ. General characteristics of optimal feed rate profiles for various fed-batch fermentation processes. *Biotechnol Bioeng*. 1986;28:1396–1407.
14. Parulekar S, Lim H. Modeling, optimization and control of semi-batch bioreactors. *Adv Biochem Eng Biotechnol*. 1985;32:207–258.
15. Rani KY, Rao R. Control of fermenters—A review. *Bioprocess Eng*. 1999;21:77–88.
16. Yu TW, Muller R, Muller M, Zhang X, Draeger G, Kim C-G, Leistner E, Floss HG. Mutational analysis and reconstituted expression of the biosynthetic genes involved in the formation of 3-amino-5-hydroxybenzoic acid, the starter unit of rifamycin biosynthesis in Amycolatopsis mediterranei S699. *J Biol Chem*. 2001;276:12546–12555.
17. Kim CG, Kirschning A, Bergon P, Zhou P, Su E, Sauerbrei B, Ning S, Ahn Y, Breuer M, Leistner E, Floss HG, Biosynthesis of 3-amino-5-hydroxybenzoic acid, the precursor of mC(7)N units in ansamycin antibiotics. *J Am Chem Soc*. 1996;118:7486–7491.
18. Moore S. Amino acid analysis—Aqueous dimethyl sulfoxide as solvent for ninhydrin reaction. *J Biol Chem*. 1968;243:6281–6283.
19. Pasqualu CR, Vigevani A, Radaelli P, Gallo GG. Improved differential spectrophotometric determination of rifamycins. *J Pharm Sci*. 1970; 59:685–687.
20. Bapat PM, Sohoni S, V, Mosses TA, Wangikar PW. A cybernetic model to predict the effect of freely available nitrogen substrate on rifamycin B production in complex media. *Appl Microbiol Biotechnol*. 2006;72:1–9.
21. Pontryagin LS, Boltyanskii VG, Gamkrelidze RV, Mishchenko EF. *The Mathematical Theory of Optimal Processes*. New York: Wiley; 1962.
22. Betts JT, Huffman P. Application of sparse nonlinear-programming to trajectory optimization. *J Guidance Control Dyn*. 1992;15:198–206.
23. Betts JT, Frank D. A sparse nonlinear optimization algorithm. *J Optim Theory Appl*. 1994;82:519–541.
24. Cervantes A, Biegler T. Large-scale DAE optimization using a simultaneous NLP formulation. *AIChE J*. 1998;44:1038–1050.
25. Cervantes AM, Wachter A, Tutuncu RH, Biegler LT. A reduced space interior point strategy for optimization of differential algebraic systems. *Comput Chem Eng*. 2000;24:39–51.
26. Binder T, Blank L, Bock HG, Bulirsch R, Dahmen W, Diehl M, Kronseder T, Marquardt W, Schlöder JP, van Stryk O. Introduction to model based optimization of chemical processes on moving horizons. In: Grötschel M, Krumke SO, Rambau J, eds. *Online Optimization of Large Scale Systems*. Berlin:Springer-Verlag; 2001:295–339.
27. Mcauley KB, Macgregor F. Optimal grade transitions in a gas-phase polyethylene reactor. *AIChE J*. 1992;38:1564–1576.
28. Ray H. *Advanced Process Control*. New York:McGraw-Hill; 1981.
29. Takeda M, Ray H. Optimal-grade transition strategies for multistage polyolefin reactors. *AIChE J*. 1999;45:1776–1793.
30. Wang Y, Seki H, Ohyama S, Akamatsu K, Ogawa M, Ohshima M. Optimal grade transition control for polymerization reactors. *Comput Chem Eng*. 2000;24:1555–1561.
31. Fletcher R. *Practical Methods of Optimization*. Chichester, UK:Wiley Ltd.; 1987.
32. Schittkowski K, Klause H.More test examples for nonlinear programming. In: *Lecture Notes in Economics and Mathematical Systems 282*. Berlin: Springer-Verlag; 1987.
33. Bapat PM, Wangikar P. Optimization of rifamycin B fermentation in shake flasks via a machine-learning-based approach. *Biotechnol Bioeng*. 2004;86:201–208.
34. Bapat PM, Das D, Dave NN, Wangikar PP. Phase shifts in the stoichiometry of rifamycin B fermentation and correlation with the trends in the parameters measured online. *J Biotechnol*. 2006; doi: 10.1016/j.jbiotec.2006.06.014.
35. Flores-Cerrillo J, MacGregor JF. Control of batch product quality by trajectory manipulation using latent variable models. *J Process Control*. 2004;14:539–553.
36. Zhang H, Lennox B. Integrated condition monitoring and control of fed-batch fermentation processes. *J Process Control*. 2004;14:41–50.

Manuscript received Dec. 26, 2005, and revision received Aug. 22, 2006.